SAND2016-9505C

Comparison of Electroluminescence Image Capture Methods

Will Hobbs[1], Olga Lavrova[2], Britny Lockridge[1]

Southern Company, Birmingham, Alabama, 35203, United States

Sandia National Laboratories, Albuquerque, New Mexico, 87125, United States

***Abstract* — In the field of photovoltaics, electroluminescence (EL) imaging has proven useful in determining the degradation of solar panels, primarily through use of expensive equipment within a confined lab setting. This study explored the potential of conducting EL imaging using relatively inexpensive equipment. Factors that heavily influenced the quality of EL images included voltage/current settings for the purpose of forward biasing the test panel, camera settings (aperture, shutter speed, and ISO), and amount of external light (not EL) detected by the camera. Once EL images were captured, the images with the best quality were analyzed and modified through image processing and photo editing. The quality of the final images was then validated through comparison with images captured in a controlled lab with higher quality equipment. Moreover, the results of transporting a solar panel are shown to be clearly observable using low-cost EL imaging.**

***Index Terms* — electroluminescence, photovoltaic cells, infrared, photocurrent, short circuit current**

I. INTRODUCTION

Vice versa to the situation of using light to generate current, photovoltaic (PV) cells generate light when supplied current. A photovoltaic cell acts like a diode or P-N junction. The photons of sunlight cause a cell to be forward biased and generate photocurrent. When a cell is forward biased by an external power source, excited electrons release energy in the form of near infrared (NIR) light. This emission of NIR light is referred to as the electroluminescence of the cell and is not visible to the human eye. However, through use of a camera that can sense infrared (IR) light, EL can provide insight into the state of “health” of photovoltaic cells. For example, EL images can show the degradation of a cell, i.e. micro-cracks, breakages, and even inhomogeneity in the crystal structure of silicon cells. Cracks and breakages, undetectable to the human eye but visible in EL images, are a common result of transporting and mishandling solar panels, and of fabrication and manufacturing defects. These images can be useful in studying the effects of PV aging or understanding the underperformance of a solar panel.

Currently, EL imaging is typically conducted in a lab setting where a solar panel can be concealed from sources of visible light, which negatively effects capture of NIR light, through use of expensive equipment. This situation is not ideal for inspecting and maintaining solar panels after installation at, e.g. a solar plant. Results from an evaluation of inexpensive and portable image capturing equipment are necessary to achieve cost-effective EL imaging in the field.

II. IMAGE CAPTURE TECHNIQUE

A. Equipment

Two panels were imaged for method evaluation purposes: a 100 W polycrystalline Solartech panel with a short circuit current (I_{SC}) of 5.72 A for laboratory testing and a 240 W polycrystalline panel with an approximate I_{SC} of 8 A. The first method of EL image capture involved the use of inexpensive equipment in the laboratory setting. An E-PL7 Olympus camera, with a Nikon lens attached via a Metabones N/F-MFT mount adapter, was initially used to capture EL images. The adapter had 0.64x magnification, resulting in a wider field of view and 1.3-stops of additional light sensitivity. As a result of requiring better low light sensitivity and a wider focus area, the Olympus camera was replaced with an ILCE-7s Sony camera with a full frame 35mm CMOS sensor. A 24mm Rokinon wide-angle lens with an f/1.4 maximum aperture was attached to this camera via an N/F- E mount mechanical adapter (with no magnification lenses). This lens allowed a wide field of view to image the panel from a relatively short distance. The IR filter covering each camera’s sensor was removed by a camera modification company, and 850 nm cutoff visible light filters were used on the front of the lenses. Test panels were forward biased using a 60 V power supply and custom made Mc4-banana plug cables. Total cost, including the power supply, was less than $5,000 for a single-camera system.

The second method of EL imaging used the same camera equipment of Method 1 in addition to a custom-made hood that could be mounted atop the fielded panel.

Fig. 1. Hood mounting on a fielded solar panel.

The third method of EL imaging used a commercially purchased Reltron EL setup, complete with a dark room, and a -20 ºC 3 stage Peltier TE cooled silicon camera with a 52 mm sensor and 35mm lens with a long-pass filter. This cooling component significantly contributed to the total cost, which was approximately an order of magnitude greater than Method 1.

B. Image Capture Methods

Method 1 consisted of the test solar panel being propped up against the back of a laboratory closet where a negligible amount of light could filter in. The camera was mounted on a tripod 9 ft. from the panel. Camera settings were adjusted by directly operating the camera. Since the Solartech panel was specifically purchased for EL image testing, the panel was supplied with enough power to generate its I_{SC} of 5.72 A to cause the panel to luminesce. The image capture technique consisted of quickly capturing sets of 10 RAW images of the test panel, alternating between being powered and unpowered. The length of time for capturing images was kept to a minimum as a precaution against overheating the test panel. The RAW images were later converted to TIFF format for processing in MATLAB. For the purpose of averaging out camera sensor and lens noise, two median images were produced in MATLAB from the 5 powered and 5 unpowered TIFF images. The two median images were then subtracted to produce an image void of noise from external light. If needed, the subtraction image was scaled to provide a better contrast between the dark and light areas of the EL image.

Method 2 involved the use of a hood composed of black corrugated sheets inserted into an extruded aluminum frame. These materials were lightweight enough for manual mounting but sturdy enough to remain stable atop a racked solar panel and support camera weight. The base of the hood was sized for a 72 cell panel, but created with inserts to function for a 60 cell panel, and had a foam rubber seal to help block out light. The aluminum frame had a mounting plate for the camera and handles for carrying; nylon straps were used to secure the hood to the PV rack. Ambient light that could leak through the back surface of the solar panel was blocked by corrugated plastic sheets fitted against the back of the panel. Once the hood was mounted and secured with straps, the Sony "Smart Remote Control" phone/tablet app was used to adjust camera settings and capture sets of 8 powered and unpowered RAW images. The panel was powered such that 90% of the panel's I_{SC}—7.53 A—could be generated. Images were processed using the same technique of Method 1.

METHOD 3 OF EL IMAGE CAPTURE SIMPLY INVOLVED SECURING THE TEST PANEL IN THE DARK ROOM AND OPERATING THE CAMERA FROM A COMPUTER THAT PROCESSED THE CAPTURED IMAGES.

III. Electroluminescence Image Comparison

Figure 2 is an EL image produced from Method 1 with the camera set to an aperture of f/2.8, shutter speed of 10 seconds, and ISO of 500. The panel contains many micro-cracks and breakages despite being newly purchased and received in protective packaging; this may be attributed to fault in the process of manufacturing. The micro-cracks are the thin crooked lines cutting through cells, and the breakages, dark spots on the cell, have been created by micro-cracks [1]. Inhomogeneity is the discoloration present in each cell. The image appears somewhat brighter in the center: this is likely a result of internal reflections in the lens.

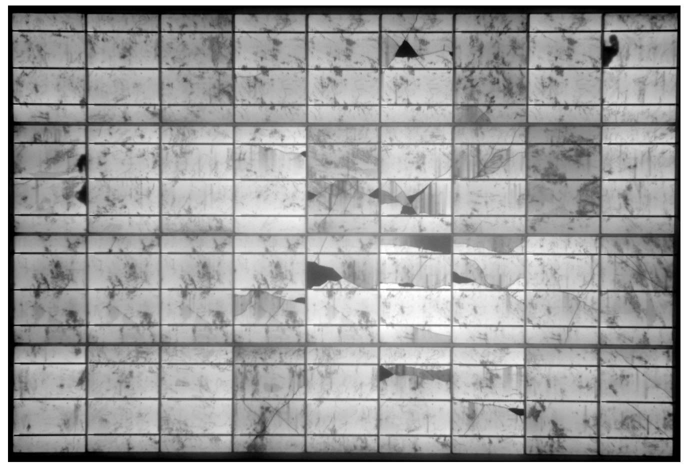

Fig. 2. EL image captured using Method 1 prior to transportation.

Figure 3 is an EL image produced from Method 3 with the camera set for a shutter speed of 1.28 milliseconds. The quality of Figure 3 is similar to that of Figure 2. Cracks, breakages, and inhomogeneity are highlighted differently due to increased contrast. Figure 3 shows more degradation than Figure 2, but this may be attributed to transportation rather than improved image quality.

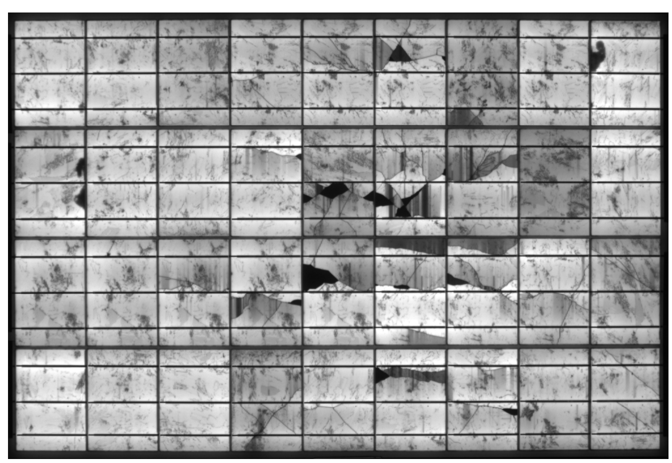

Fig. 3. EL image captured using Method 3 after transportation.

Figure 4 is the EL image acquired in the same setting as Figure 3 using the camera equipment of Method 1 with the camera set to an aperture of f/4.0, shutter speed of 10 seconds, and ISO of 1000 while the panel was supplied 5 A of current for powered images. The brighter center is once again most likely an effect of internal reflections in the lens

Fi ... ng M

... 3 ... EL
im ... am ... nd
br ... s to ... ges
fr ... y th ... on
ga ... . I ... up
co ... whe ... els
w ... rom ... of
M

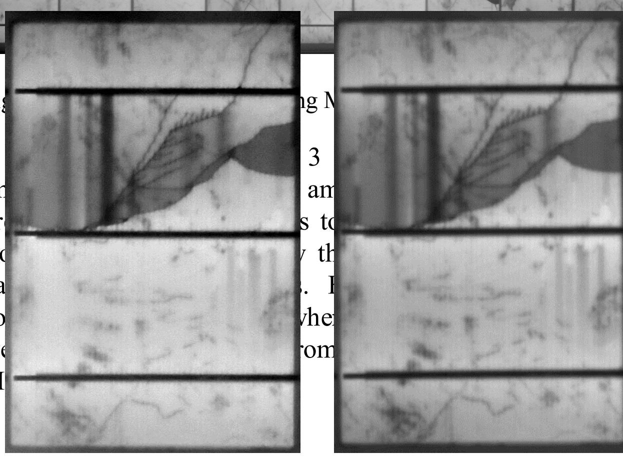

Fig. 5. Close-up comparison of a single cell from Method 1 (left) and Method 3 (right).

Figure 6 displays a close up of the effect of transportation on a cell that experienced the most damage. The after-transportation close-up exhibits far more cracks and breakages than the before image. EL is not present in these areas because no current exists; this suggests power loss within the cell. Thus, the damage inflicted by transportation and possible mishandling of the panel is emphasized by EL images. This comparison of results from Methods 1 and 3 validates the use of low-cost equipment for procuring information regarding the condition of the cell.

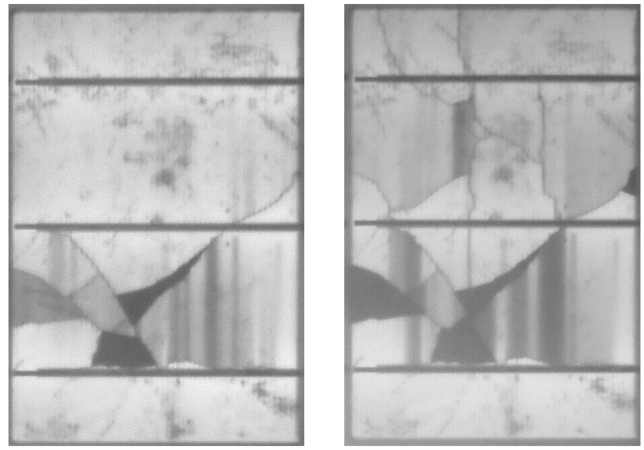

Fig. 6. Before (left) and after (right) EL images displaying effects of transportation on a photovoltaic cell.

IV. EL IMAGING IN THE FIELD

Figure 7 shows an EL image of the fielded panel described above using Method 2 with the following camera settings: an aperture of f/1.4, shutter speed of 3.2 seconds and ISO of 2000. While not as sharp as the images captured in the lab setting, this EL image does show characteristics of the panel. For example, cell inhomogeneity is evident, and three cells stand out darker than the rest of the cells. The darker output may imply low energy conversion efficiency. While the bottom and top right edges of the panel appear dark, this should not be mistaken for conversion inefficiency; the darkness is a result of image processing on un-wanted NIR leaking through the base of the solar panel hood. To minimize NIR light leakage, a tighter seal between the foam rubber and panel is needed, in addition to between the corrugated plastic sheets and aluminum frame of the hood.

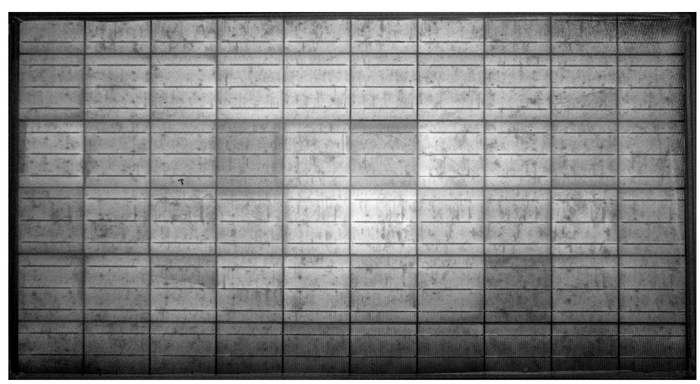

Fig. 7. EL image captured using Method 2 on the fielded panel.

A micro-crack, shown in Figure 8, is present in the third column from the left and second row from the bottom of the panel (left cell) as well as the second column from the right and second row from the top of the panel (right cell). The portion of the left cell above the crack is slightly darker than the portion below the crack. This may imply low energy conversion efficiency as well. The identical brightness of the portions below and above the micro-crack in the right cell suggests the micro-crack in the left cell is worse than that in the right cell.

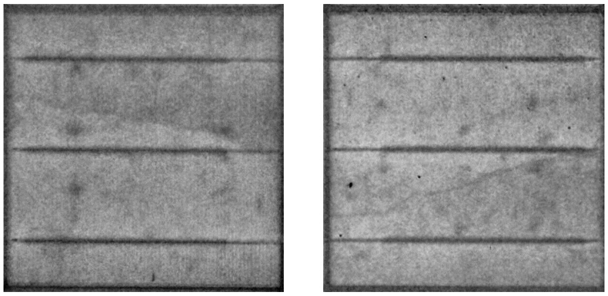

FIG. 8. MICRO-CRACKS PRESENT IN THE FIELDED PANEL.

IV. ADDITIONAL IMAGING TECHNOLOGIES

An additional imaging technique that has been explored superposes EL and IR imaging. An example of an IR image is shown in Figure 9.

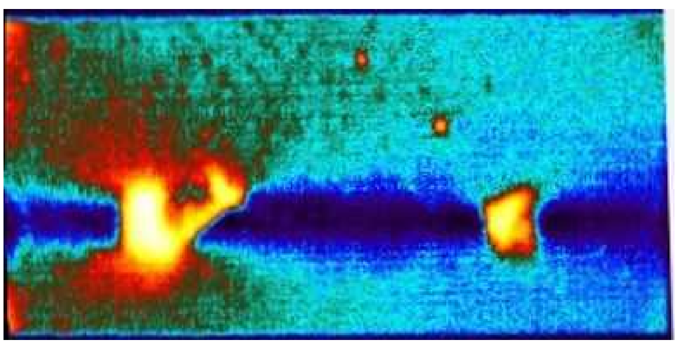

Fig. 9. An IR image of a PV panel

Figure 10 presents this same IR image overlaid with EL. Overlay of IR and EL images allows for more accurate interpretation of the results and more precise spatial location of defects or damages within PV panel or cell. Further results of imaging capabilities will be presented at the time of the conference.

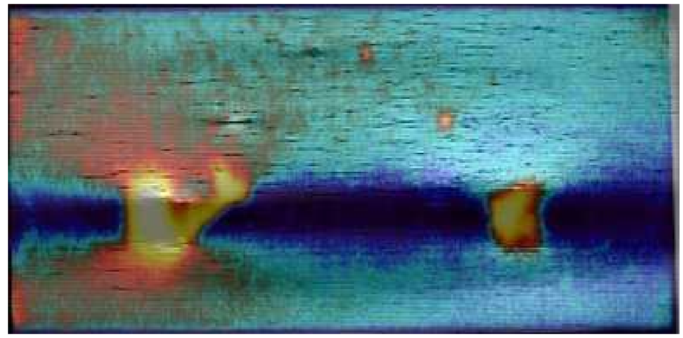

Fig. 10. An optical image of a PV panel consisting of a superposition of IR and EL images

VI. CONCLUSION

The EL images captured with the low-cost equipment and the high-cost equipment were comparable in presentation of micro-cracks, breakages, and inhomogeneity. Difference in image quality was primarily attributed to differing image processing techniques. The effects of transportation were apparent in the results of both Methods 1 and 3 in which an increase in micro-cracks and breakages was observed. The observation of panel characteristics in the results of Method 2 proved the success of field imaging using low-cost equipment, while additionally highlighting areas for equipment improvement. The result and advantages of overlaying an IR image with EL were presented. In conclusion, this paper aims to aid researchers in realizing the full potential of EL imaging.

ACKNOWLEDGEMENT

The authors would like to thank Southern Research for their assistance with field imaging, in addition to Charles Robinson from Sandia National Laboratories, who provided training with the Reltron EL setup as well as the IR and IR with EL overlay images.

Sandia National Laboratories is a multi-program laboratory managed and operated by Sandia Corporation, a wholly owned subsidiary of Lockheed Martin Corporation, for the U.S. Department of Energy's National Nuclear Security Administration under contract DE-AC04-94AL85000.

THIS WORK WAS SUPPORTED IN PART BY THE DOE AWARD DE-FOA-0001195-1508.

…REFERENCES

[1] A. Mansouri, et al., "Defect detection in photovoltaic modules using electroluminescence imaging," in *27th European Photovoltaic Solar Energy Conference*, 2012 © EU PVSEC. doi: 10.4229/27thEUPVSEC2012-4BV.2.45